

Genome-wide DNA hypomethylation shapes nematode pattern-triggered immunity in plants

Mohammad Reza Atighi^{1*} , Bruno Verstraeten^{1*}, Tim De Meyer^{2†}  and Tina Kyndt^{1†} 

¹Department of Biotechnology, Ghent University, B-9000, Ghent, Belgium; ²Department of Data Analysis & Mathematical Modelling, Ghent University, B-9000, Ghent, Belgium

Author for correspondence:

Tina Kyndt

Tel: +32 9 264 5920

Email: tina.kyndt@ugent.be

Received: 4 October 2019

Accepted: 26 February 2020

New Phytologist (2020) 227: 545–558

doi: 10.1111/nph.16532

Key words: basal defence, DNA hypomethylation, *Meloidogyne graminicola*, nematodes, *Oryza sativa*, pattern-triggered immunity, RdDM, rice.

Summary

- A role for DNA hypomethylation has recently been suggested in the interaction between bacteria and plants; it is unclear whether this phenomenon reflects a conserved response.
- Treatment of plants of monocot rice and dicot tomato with nematode-associated molecular patterns from different nematode species or bacterial pathogen-associated molecular pattern flg22 revealed global DNA hypomethylation. A similar hypomethylation response was observed during early gall induction by *Meloidogyne graminicola* in rice. Evidence for the causal impact of hypomethylation on immunity was revealed by a significantly reduced plant susceptibility upon treatment with DNA methylation inhibitor 5-azacytidine.
- Whole-genome bisulphite sequencing of young galls revealed massive hypomethylation in the CHH context, while not for CG or CHG nucleotide contexts. Further, CHH hypomethylated regions were predominantly associated with gene promoter regions, which was not correlated with activated gene expression at the same time point but, rather, was correlated with a delayed transcriptional gene activation. Finally, the relevance of CHH hypomethylation in plant defence was confirmed in rice mutants of the RNA-directed DNA methylation pathway and DECREASED DNA METHYLATION 1.
- We demonstrated that DNA hypomethylation is associated with reduced susceptibility in rice towards root-parasitic nematodes and is likely to be part of the basal pattern-triggered immunity response in plants.

Introduction

There is mounting evidence that epigenetic mechanisms, such as DNA methylation, play an important role in plant development and response to adverse environmental conditions (Pikaard & Mittelsten Scheid, 2014). In plants, *de novo* methylation is catalysed by DOMAINS REARRANGED METHYLTRANSFERASE (DRM2) and maintenance is performed by three classes of enzymes: CG methylation is maintained by methyltransferase 1, CHG methylation by plant-specific chromomethylases (CMT2 and CMT3), and CHH methylation by DRM2 or CMT2 depending on the genomic region (Chan *et al.*, 2005; Law & Jacobsen, 2010; Zhang *et al.*, 2018). The RNA-directed DNA methylation (RdDM) pathway, a plant-specific small-RNA (smRNA)-triggered pathway, guides DRMs to target sequences (Matzke & Moshier, 2014). In the canonical RdDM pathway, RNA polymerase IV generates single-stranded RNA molecules, which are used as a template for RNA-DEPENDENT RNA POLYMERASE 2 to generate double-stranded RNA (dsRNA).

In Arabidopsis, but largely conserved among plants (Haag and Pikaard, 2011), these dsRNAs are trimmed by DICER LIKE 3 (DCL3) to 24-nt small interfering RNAs (siRNAs), methylated

by HUA ENHANCER 1, and loaded onto ARGONAUTE 4 (AGO4) of the RNA-induced silencing complex. DNA unwinds at the target site by the DNA-dependent RNA polymerase V (DDR) complex, upon which RNA polymerase V transcribes an RNA scaffold, which base-pairs with AGO4-bound siRNA, enabling DRM2 to establish *de novo* methylation (Matzke & Moshier, 2014; Zhou *et al.*, 2018). Transposable elements (TEs) can be part of RdDM as a source of smRNAs (Slotkin & Martienssen, 2007; Lisch, 2009; Zakrzewski *et al.*, 2017). CHH methylation can also be facilitated by DECREASED DNA METHYLATION 1 (DDM1), catalysed by CMT2, independent of RdDM (Zemach *et al.*, 2013). Together, DDM1 and RdDM synergistically mediate the majority of transposon methylation and methylation-dependent regulation of gene expression in Arabidopsis (Zemach *et al.*, 2013).

DNA methylation controls many genes involved in key processes in plants (Law & Jacobsen, 2010; Deleris *et al.*, 2016). Plant immunity comprises two tiers: pattern-triggered immunity (PTI) and effector-triggered immunity (ETI). PTI is triggered when the presence of a pathogen-associated molecular pattern (PAMP) or a damage-associated molecular pattern (DAMP) is perceived by pattern recognition receptors. The second layer is triggered by pathogen-secreted effector molecules that target PTI suppression, yet can be recognized by nucleotide-binding

*†These authors contributed equally to this work.

leucine-rich repeat proteins, resulting in isolate-specific defence responses (Jones & Dangl, 2006; Zipfel, 2014). DNA methylation was suggested to be involved in the plant immune response to bacterial pathogens. Infection of *Arabidopsis* with bacterial pathogen *Pseudomonas syringae* pv *tomato* DC3000 leads to hypomethylation in genomic regions associated with plant defence genes (Pavet *et al.*, 2006) and at (peri)centromeric regions, whereas methylation-deficient mutants are less susceptible to this pathogen (Pavet *et al.*, 2006). Hypomethylated *Arabidopsis* mutants are more resistant to oomycete biotrophic pathogen *Hyaloperonospora arabidopsidis*, but not to necrotrophic pathogen *Plectosphaerella cucumerina* (López Sánchez *et al.*, 2016). An *Arabidopsis* triple mutant in DNA demethylases (*rdm1/dml2/dml3*) showed increased susceptibility to infection by *Fusarium oxysporum* through deregulation in expression of TE-containing defence-related genes (Le *et al.*, 2014). Most studies so far have focused on the model plant *Arabidopsis*, whereas studies on other plants are lagging behind. In rice (*Oryza sativa*), chemical demethylating agents were found to reduce susceptibility towards *Xanthomonas oryzae* pv *oryzae* (Akimoto *et al.*, 2007). These results suggest a role for DNA methylation in plant defence, though only aboveground tissues were investigated. It remains unclear whether this process works across multiple tissue types and genome-wide, whether it is involved in PTI and/or ETI, or whether the reported methylation changes are merely the consequence of targeted effector-based manipulation of the PTI response. Moreover, the functional genomic context, cytosine context, and relationship to TE expression remains to be elucidated. Treatment of *Arabidopsis* with flg22, a bacterial PAMP, induces hypomethylation in *Arabidopsis* and restricts bacterial propagation (Yu *et al.*, 2013), which suggests hypomethylation to be a PTI response. If true, one would expect a broad range of inducing pathogens/PAMPs, as well as evolutionary conservation, and a tissue-independent response.

Here, we focus on the impact of a belowground pathogen, parasitic nematodes, on the monocot model plant rice. The root-knot nematode *Meloidogyne graminicola* is one of the most damaging nematodes attacking monocots (Bridge *et al.*, 2005). Moreover, we evaluate whether we see similar effects in tomato in interaction with the most damaging root-knot nematode that attacks dicots, *Meloidogyne incognita*. Generally understudied due to their belowground symptoms, parasitic nematodes cause major yield losses, certainly in crops like rice (Bridge *et al.*, 2005) and tomato (*Solanum lycopersicum*) (Sasser & Carter, 1985). Sedentary cyst and root-knot nematodes maintain an intimate biotrophic relationship with their host, during which a specialized feeding site is formed (syncytia and galls, respectively). Detailed messenger RNA and smRNA-sequencing efforts have demonstrated activation of epigenetic mechanisms upon nematode infection (Hewezi *et al.*, 2008; Li *et al.*, 2012; Ji *et al.*, 2013; Portillo *et al.*, 2013; Cabrera *et al.*, 2016; Medina *et al.*, 2018) and accumulation of heterochromatic 24-nt siRNAs, which were found to be associated with hypermethylation of TEs and gene promoters in syncytia (Hewezi *et al.*, 2017). However, whole-genome bisulphite sequencing (WGBS) on soybean roots infected with *Heterodera glycines* revealed overrepresentation of hypomethylated regions, and it is

currently unknown whether DNA methylation changes are elicited by the pathogen or are part of a plant defence response (Rambani *et al.*, 2015). A recently discovered nematode-PAMP (nematode-associated molecular pattern, or NAMP) called 'NemaWater', activates an early PTI response in plants, a phenomenon that is correlated with hydrogen peroxide (H₂O₂) accumulation (Mendy *et al.*, 2017). Evaluating the impact of nematode infection, but also NemaWater, on DNA methylation in plant roots may shed light on the question of whether hypomethylation is a general plant defence mechanism or a consequence of pathogen effectors that induce feeding site formation.

Here, we investigated the role of DNA methylation in the interaction between host plants and parasitic nematodes. Treatment of rice and tomato with different NAMPs from nematodes with varying lifestyles provides the first insight into the role of DNA hypomethylation in the PTI response upon nematode attack in roots. We also provide evidence that a similar hypomethylation response is induced upon application of bacterial PAMP flg22. By further focusing on the interaction between rice and *M. graminicola*, by WGBS, gene expression analysis, infection assays on mutants, and 5-azacytidine treatment, we provide detailed insights in the genomic contexts targeted by hypomethylation and evidence for a causal impact of DNA hypomethylation on plant defence against nematodes.

Materials and Methods

Plant growth and treatments

Oryza sativa L. cv Nipponbare (GSOR-100, USDA) seeds were germinated for 5 d in darkness at 30°C, after which they were transferred to synthetic absorbent polymer substrate in polyvinylchloride tubes (Reversat *et al.*, 1999) and grown at 28°C (16 h : 8 h, light : dark). Two-week-old plants were inoculated by 250 stage juvenile (J2) of *M. graminicola* per plant or mock inoculated with water as a control. After 36 h, they were transferred to 50% Hoagland solution in glass tubes to synchronize infection. Three days later, galls of infected plants and root tips of control plants were harvested and frozen in liquid nitrogen (N₂).

Tomato seeds (cv Moneymaker) were germinated in potting soil at 24°C. Two-week-old rice and tomato plants were sprayed and root-drenched in NAMP (see below) or PAMP (1 µM flg22; Eurogentec, Liege, Belgium) or water as mock treatment under hydroponic conditions for 36 h, after which they were washed and transferred to 50% Hoagland solution. A sterile culture of *Pratylenchus zeae* was maintained on carrot disks. A culture of *M. incognita* and one of *M. graminicola* was maintained on susceptible host plants in potting soil. Rice plants were treated by spraying and root drenching with NAMP obtained from *M. graminicola* or *P. zeae*, whereas tomato plants were treated with NAMP obtained from *M. incognita*. NAMP (NemaWater) was prepared by shaking c. 30 000 J2 nematodes in 150 ml of water (100 rpm) overnight at room temperature and subsequent filter sterilization of the supernatant through a 0.22 µm filter (Mendy *et al.*, 2017).

In one experiment, we first sterilized the nematodes using four antibiotics (carbenicillin, gentamycin, kanamycin, and spectinomycin, each $200 \mu\text{g ml}^{-1}$) plus Hospital Antiseptic Concentrate ($3.3 \mu\text{l ml}^{-1}$) for 1 h, after which the nematodes were thoroughly rinsed.

Enzyme-linked immunosorbent assay-based global DNA methylation assay and hydrogen peroxide quantification

For the enzyme-linked immunosorbent assay (ELISA)-based tests, DNA from 3 d post-inoculation (dpi) galls or root at 3 d post-NAMP treatment and their corresponding mock-treated control samples was extracted using the cetyltrimethylammonium bromide (CTAB) method (Doyle & Doyle, 1987) and quantification was performed using NanoDrop 2000 (Thermo Fisher Scientific, Waltham, MA, USA). Global DNA methylation was quantified using the 5-methylcytosine (5-mC) DNA ELISA kit (Zymo Research, Irvine, CA, USA) using highly specific 5-mC antibodies for any DNA context (CG, CHG or CHH) according to the manufacturer's protocol. For each treatment, at least 10 biological replicates were measured, with two technical replicates for each. One biological replicate was composed by extracting DNA from the pooled material of at least 20 individual plants.

H₂O₂ measurements were performed as previously described (Khanam *et al.*, 2018). Plants were treated with NemaWater, as described earlier. Thirty-six hours later, they were transferred to 50% Hoagland solution, and material was harvested after an additional 36 h. For each treatment, four biological replicates (pool of five plants) and two technical replicates were measured.

Infection assays on RNA-directed DNA methylation mutants and 5-azacytidine-treated plants

Thirteen-day-old rice plants were sprayed with different concentrations of 5-azacytidine, whereas control plants were mock sprayed with water; both solutions contained 0.02% (v/v) Tween 20 as a surfactant (Latzel *et al.*, 2016; Puy *et al.*, 2018; Münzbergová *et al.*, 2019). The next day, plants were inoculated with 250 J2 of *M. graminicola*.

Rice mutants were kindly provided by other laboratories: *dcl3a* and *dcl3b* mutants by Cao's laboratory (Song *et al.*, 2012), *ago4a/b* mutant by Qi's laboratory (Wu *et al.*, 2010), *drm2* and *ddm1* double mutant by Zhou's laboratory (Tan *et al.*, 2016), and *waf1* mutant by Itoh's laboratory (Abe *et al.*, 2010). These mutants do not have a root growth phenotype.

Two-week-old plants were inoculated, and 2 wk later the roots were harvested and stained by boiling in 0.013% acid fuchsin for 3 min. The number of galls and nematodes were counted under a SMZ1500 stereomicroscope (Nikon, Melville, NY, USA).

DNA extraction, library preparation, and whole-genome bisulphite sequencing

About 200 mg of 3 dpi *M. graminicola* galls collected from *c.* 100 plants and corresponding control root-tip material were ground

to a fine powder by mortar and pestle in liquid N₂. For both galls and root tips (three biological replicates per condition), DNA was extracted using the DNeasy plant mini kit (Qiagen) according to manufacturer's instructions and dissolved in DNase-free water. DNA concentration was quantified using the Quant-it PicoGreen dsDNA Assay kit (Thermo Fisher Scientific), and 100 ng of DNA per sample was sheared to 400 bp fragments using a Covaris S2 Focused-ultrasonicator (Covaris, Woburn, MA, USA). Sonicator settings were duty cycles of 10%, intensity of 4, and cycles/burst of 200 for 65 s. Fragmented DNA was cleaned and concentrated using the DNA clean and concentrator kit (Zymo Research). Bisulphite conversion was performed by the EZ DNA methylation Gold kit (Zymo Research). Bisulphite conversion efficiency was evaluated by spiking each sample with Lambda unmethylated DNA (0.5% of total DNA in sample) prior to shearing, leading to an efficiency estimate of > 99% for all samples (Supporting Information Table S1). Size distribution was verified using the high-sensitivity DNA chip of a Bioanalyzer 2100 instrument (Agilent Technologies, Santa Clara, CA, USA).

The preparation of sequencing libraries from bisulphite-converted DNA was performed using the Accel-NGS Methyl-Seq DNA library kit according to manufacturer's instructions (Swift Biosciences, Ann Arbor, MI, USA). DNA quality was checked again using the high-sensitivity DNA chip of the Bioanalyzer 2100 instrument (Agilent Technologies). After gel purification, quantitative PCR (qPCR) was performed to determine the concentration of each sample. A 2.1 pM library was loaded on the flow cell and sequenced using an Illumina Nextseq500 (single end, 76 cycles).

Whole-genome bisulphite sequencing data analysis

Reads were trimmed with TRIM GALORE (v.0.4.0) using default settings. Trimmed reads were mapped against the *O. sativa* subsp. *japonica* reference genome (build MSU7.0) with BISMARK software (v.0.18.1_dev) using the following parameters: bowtie2; q; un; score_min L,0,0.3; p 4 (Krueger & Andrews, 2011). The resulting SAM files were converted to BAM format and sorted. Files were demultiplexed using SAMTOOLS (v.1.3). Duplicate reads were removed using PICARD (v.1.119). Per sample, coverage files containing methylated and unmethylated read counts were extracted using the BISMARK (Krueger & Andrews, 2011) methylation extractor for every cytosine context, imported in R (v.3.5.0) with the read.bismark function (BSSEQ package, 1.18.0) using the following parameters: rmZeroCov = TRUE and strandCollapse = FALSE. This was used as input for DMRSEQ (v.1.0.14; Korthauer *et al.*, 2018) to identify differentially methylated regions (DMRs) per cytosine context (three gall samples vs three uninfected root tips). Default settings were used except when mentioned otherwise.

Cytosines without any read in any sample were filtered out before analysis. DMRs with an FDR (Benjamini-Hochberg procedure) < 0.05 were considered significant. Promoters were defined as regions 2000 bp upstream of the transcription start site. The Rice Annotation Project-Database (RAP-DB) IDs of these gene lists were used as input for Gene Ontology (GO) overrepresentation

tests by PANTHER (Mi *et al.*, 2017). GO analysis was performed on three sets of genes: the 'promoter set', containing all genes that exclusively overlap with DMRs through their promoters; the 'gene body set', containing all genes that exclusively overlap with DMRs through their gene bodies; and the 'combination set', containing all genes that overlap with DMRs through both promoter and gene body regions. MAPMAN 3.5.1R2 pathway analysis was performed on these lists by means of Wilcoxon rank-sum tests.

RNA-sequencing data analysis

Differentially expressed genes in 3 dpi and 7 dpi *M. graminicola* galls vs uninfected root tips were already available (Kyndt *et al.*, 2012) from previous research by our group under similar experimental conditions. The dataset (GEO accession no. PRJNA151855) was reanalysed to monitor TE-expression profiles. Reads were trimmed with TRIMMOMATIC (v.0.36; Bolger *et al.*, 2014) and mapped against the *O. sativa* subsp. *japonica* reference genome (build MSU7.0) using STAR (v.2.5.2a; Dobin *et al.*, 2013). Only uniquely mapped reads were kept for further analysis. BAM files of multiplexed samples were merged using SAMTOOLS (v.1.3). Count tables were generated by the summarizeOverlaps function in the GENOMICALIGNMENTS R package (v.1.16.0; Lawrence *et al.*, 2013). Differential expression analysis was performed using the DESeq2 package (v.1.20; Love *et al.*, 2014) with TE annotations found in the Rice Transposable Element database (Copetti *et al.*, 2015). TEs with a false discovery rate (FDR) < 0.05 were considered differentially expressed (DE) compared with the control group (uninfected root tips). Significance of the expression trends of gene sets DE at 3 or 7 dpi was ascertained by two-sided binomial tests with a success probability (under the null hypothesis) of 0.5.

Association between differentially methylated regions and genomic regions

To assess significance of overlap between DMRs, gene bodies, and TEs, the REGIONER package (v.1.14.0) was used (Gel *et al.*, 2016). Permutation tests were performed whereby promoter regions, gene body regions, and TE regions were randomly scattered across the genome and the number of overlaps with DMRs was counted. Enrichment of DE genes and TEs at either 3 or 7 dpi in the DMRs was also assessed. To account for association bias between genes or TE classes with DMRs, per permutation, a set of genes/TEs of equal size to the set of DE genes was randomly selected from the total set of rice genes/TEs and the overlap with DMRs was counted. Similarly, enrichment of hypomethylated TEs in gene promoters was assessed: a set of TEs of equal size to the set of hypomethylated TEs was randomly selected from the total set of rice TEs and the overlap with gene promoters was counted. For all tests, 1000 permutations were performed to create a null distribution, and a *P*-value significance threshold of 0.05 was maintained. GO analysis was performed with AGRIGO v.2, in Singular Enrichment Analysis mode, using all rice genes as a reference background. GO visualization was done using REVIGO (Supek *et al.*, 2011; Tian *et al.*, 2017).

Quantitative reverse transcription PCR and chop-quantitative PCR

Meloidogyne graminicola galls and corresponding control root tips at 3 and 7 dpi were collected for three biological replicates each. RNeasy Mini Kit (Qiagen) was used to extract RNA from root samples following the manufacturer's protocol by additional sonication after adding RLT buffer. RNA was quantified using a NanoDrop 2000 instrument (Thermo Fisher Scientific). First-strand complementary DNA (cDNA) was synthesized using Tetro Reverse Transcriptase (Bioline, Memphis, TN, USA). The quality of cDNA was checked using reference genes by PCR. All quantitative reverse transcription (qRT) PCRs were performed in triplicate. qPCR conditions consisted of an initial denaturation at 95°C for 10 min, followed by 50 cycles of denaturation at 95°C for 25 s, annealing at 58°C for 25 s, and extension at 72°C for 20 s. The data obtained were analysed using REST 2009 software. Expression data were normalized using data of two reference genes (Kyndt *et al.*, 2012). The relative expression level is shown as the log₂-fold change in transcript level compared with control samples.

For chop-qPCR, DNA was extracted with CTAB as described earlier. The chop protocol of Dasgupta & Chaudhuri (2019) was followed using *AluI* or *DdeI* and a digestion time of 1 h, after which qPCR was executed using identical conditions to those already described.

The primers used in this study are listed in Table S2.

Data availability

Data generated in this study were deposited in Gene Expression Omnibus under accession no. GSE130064. Gene and TE expression data were obtained with published data sets (accession no. PRJNA151855, specifically samples with accession nos. GSM876135–GSM876140 and GSM876145–GSM876150).

Further statistical analyses

For further statistical analyses, SPSS (v.25; IBM, Armonk, NY, USA) and R (v.3.5.0) were used where relevant; normality of data was checked using a Kolmogorov–Smirnov test ($\alpha = 0.05$), and homoscedasticity using the Levene test ($\alpha = 0.05$). Where necessary, a nonparametric test (Mann–Whitney) was applied.

Results

DNA hypomethylation is part of a pattern triggered immunity response upon root-knot nematode infection

First, we investigated methylome changes in rice roots upon infection by root-knot nematode *M. graminicola*. An ELISA-based experiment was conducted on galls and corresponding uninfected root tips at 3 dpi, a time point where early giant-cell formation is observable in rice (Mantelin *et al.*, 2017). The analyses showed strong hypomethylation in young galls induced by nematodes (Fig. 1a).

We hypothesized that hypomethylation is a general plant defence response, rather than being instigated by the nematode. To prove this hypothesis, 5-azacytidine, an inhibitor of DNA methyltransferases, was sprayed (Gonzalez *et al.*, 2016; Latzel *et al.*, 2016; Puy *et al.*, 2018; Münzbergová *et al.*, 2019) on plants 24 h before nematode inoculation. To rule out direct effects on the nematodes, we executed foliar application. Note that Puy *et al.* (2018) showed that spraying 5-azacytidine has the same efficiency as seed treatment with a smaller retardation effect on plant development. Gonzales *et al.* (2016) showed that spraying 5-azacytidine leads to a global DNA methylation reduction in *Trifolium repens* at 50 μM concentration. Four different concentrations (300, 100, 75, and 50 μM) were applied, but the two highest concentrations caused strong developmental defects on the plants and were hence not used further. Spraying with 50 μM 5-azacytidine caused no developmental defects, but upon application of 75 μM 5-azacytidine the shoots were significantly shorter (Figs 1b, S1). Upon 50 μM 5-azacytidine treatment, a significant reduction in methylation was detected in roots (Fig. S2). For both 50 and 75 μM 5-azacytidine, a significantly lower number of galls and nematodes (decreases of c. 25–30%, all $P < 0.05$) was observed compared with control plants, endorsing the hypothesis that DNA hypomethylation reduces susceptibility of plants against root-knot nematodes (Figs 1b, S1). We also compared number of females per gall in control vs treated plants and found no significant difference (Fig. S3). Together, this indicates that DNA hypomethylation is part of the early plant defence mechanism that precludes nematode invasion and/or feeding site development, rather than being a consequence of nematode infection and feeding site formation.

To further confirm the hypothesis that DNA hypomethylation is a PAMP-triggered immunity response, we investigated the effect of treatment with a NAMP on the methylome of plants. NAMPs from two groups of nematodes with diverging lifestyles (sedentary and migratory) were applied on two different host plants: sedentary root-knot nematodes *M. graminicola* (on rice), and *M. incognita* (on tomato) and migratory nematode *P. zeae* (on rice). ELISA-based quantification revealed

strong DNA hypomethylation (relative decreases of 65%, 86%, and 50%, respectively, all $P < 0.05$) of roots in NAMP-treated plants in both rice and tomato compared with the mock-treated plants (Fig. 2a–c). To confirm and extend previous observations of DNA hypomethylation upon bacterial PAMP treatment in *Arabidopsis* (Yu *et al.*, 2013), rice and tomato plants were sprayed with 1 μM of flg22, and significant DNA methylation reduction was observed in both rice and tomato (Fig. 2d–e), similar to the results obtained by application of 5-azacytidine on rice (Fig. S2).

These NAMPs/PAMPs were shown to induce PTI marker genes in rice (De Kesel *et al.*, 2020). The biological activity of NemaWater was also evaluated by investigating induction of reactive oxygen species (ROS), a hallmark for PTI responses. As previously shown (Mendy *et al.*, 2017), NemaWater induced production of ROS in a concentration-dependent manner in rice. Moreover, it remained active when the nonsterile *M. graminicola* nematodes used to generate NemaWater were pretreated with antibiotics to remove potential bacteria (Table S3).

These observations indicate that DNA hypomethylation is part of a conserved PTI response in monocot and dicot plants.

Whole-genome bisulphite sequencing supports a central role for CHH hypomethylation

To further study the functional and nucleotide context of the observed hypomethylation, we decided to focus on the rice–*M. graminicola* model system, for which genome-wide expression data have previously been generated by our research group, under similar experimental conditions (Kyndt *et al.*, 2012). DNA methylation analysis was performed by WGBS on 3 dpi galls compared with uninfected control root tips. Three replicates were used per condition, and a total of 332.6 million reads were generated (see Table S1 for more details). Mapping against the *M. graminicola* genome (Somvanshi *et al.*, 2018) resulted in mapping rates of 1.1% (galls) and 0.1% (uninfected root tips), indicating that their presence in our reads is negligible and that we have almost exclusively extracted plant DNA.

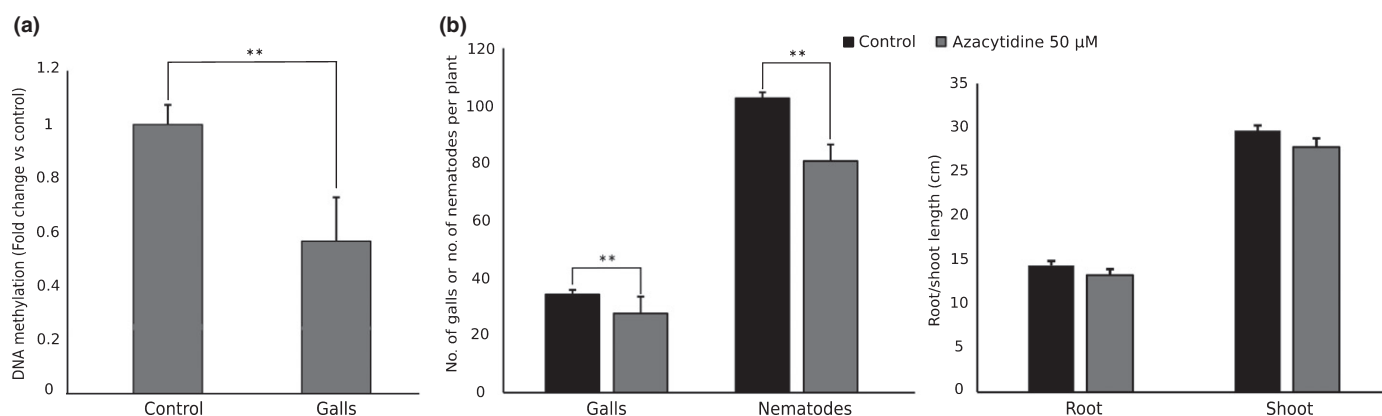


Fig. 1 Nematode (*Meloidogyne graminicola*) infection causes strong hypomethylation in rice plants, which is associated with plant defence. (a) Enzyme-linked immunosorbent assay reveals global DNA hypomethylation upon nematode infection in young (3 d post-inoculation) galls induced in rice roots ($n = 12$). (b) Foliar application of 5-azacytidine (50 μM) 24 h before nematode inoculation makes plants less susceptible to nematode infection, while root and shoot length were unaffected ($n = 20$); galls and nematodes were counted 2 wk post-inoculation. *, $P < 0.1$; **, $P < 0.05$. Error bars indicate SEM.

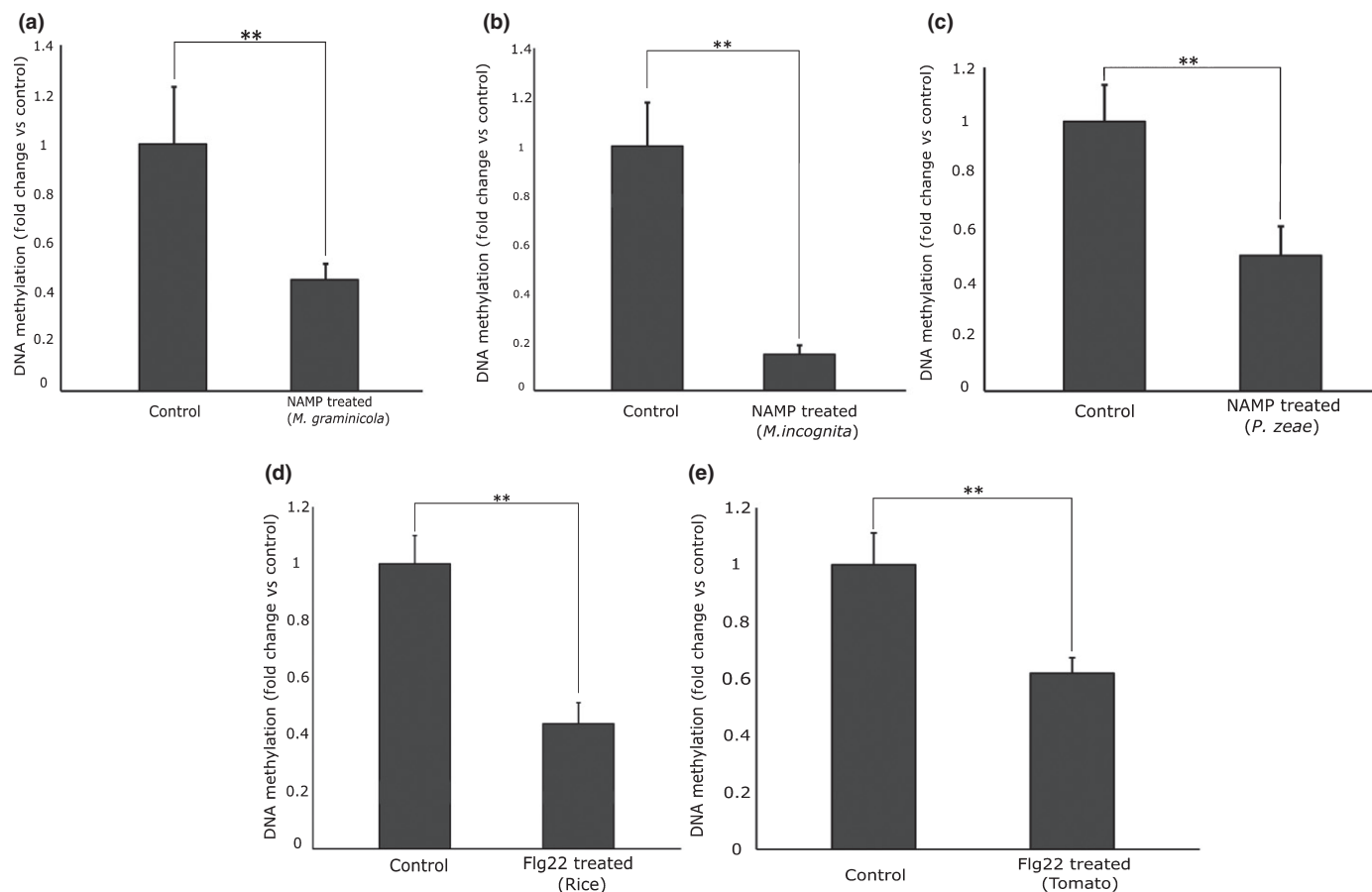


Fig. 2 Nematode-associated molecular pattern (NAMP) and bacterial pathogen-associated molecular pattern (PAMP) treatments cause strong hypomethylation in plants 3 d post-treatment. (a) Treatment of rice plants with NAMP obtained from *Meloidogyne graminicola* compared with untreated plants ($n = 9$). (b) Treatment of tomato plants with NAMP obtained from *Meloidogyne incognita* compared with untreated plants ($n = 10$). (c) Treatment of rice plants with NAMP obtained from *Pratylenchus zeae* compared with untreated plants ($n = 10$). (d) Treatment of rice plants with bacterial PAMP (flg22) compared with untreated plants. (e) Treatment of tomato plants with bacterial PAMP (flg22) compared with untreated plants. *, $P < 0.1$; **, $P < 0.05$. Error bars indicate SEM. flg22, flagellin 22.

Comparing overall DNA methylation patterns, both genome-wide and specifically of genic and TE regions, a clear decrease in CHH methylation was observed in galls, whereas CG and CHG methylation remained stable (Fig. 3a). Subsequently, we searched for local differences between galls and roots, leading to a total of 9677 DMRs (FDR < 0.05 ; Table S6). DMRs are not clustered on a specific chromosome, but DMR distribution per chromosome shows a decrease in centromeric regions for all chromosomes (Fig. 3b). Grouped per nucleotide context, 23, 0 and 9654 DMRs were found in CG, CHG and CHH contexts, respectively.

Though there was an almost even split of CG DMRs in terms of hypo/hypermethylation, 99.97% of CHH DMRs were hypomethylated in galls vs control tissue, indicating a significant role for CHH hypomethylation in response to *M. graminicola* infection (Fig. 4a). CHH hypomethylation in *M. graminicola* galls was independently assessed by chop-qPCR for three loci (Table S4).

As an exploratory analysis, enrichment testing was done using definitions as outlined in the Materials and Methods section (WGBS data analysis). CG DMRs were not significantly

positively or negatively associated with gene body regions or promoter regions. However, CHH DMRs were significantly negatively associated with gene body regions (18% less than expected, $P < 0.001$), whereas they were significantly positively associated with promoter regions (64% more than expected, $P < 0.001$; Fig. 4b). GO analysis applied on promoter, gene body, and combined DMRs showed clear enrichment for GO terms 'metabolic processes' and 'stress response' for genes associated with promoter DMRs, whereas results for gene body DMRs were less outspoken (Fig. S4). MAPMAN pathway analysis (Thimm *et al.*, 2004) showed no significant enrichment for any specific pathway among the DMRs, whether they were associated with promoter or gene body regions.

We evaluated whether DMRs are located in TEs. Based on the Rice TE database (Copetti *et al.*, 2015) TEs are categorized in five classes: DNA transposon Mutator (DTM), Retroelement long tandem repeat Gypsy (RLG), Retroelement long tandem repeat Copia (RLC), Retroelement long tandem repeat 'Unknown' (RLX), and Retroelement short interspersed nuclear elements (RSU), in the Rice Transposable Element database (Copetti *et al.*, 2015). CG DMRs were not significantly

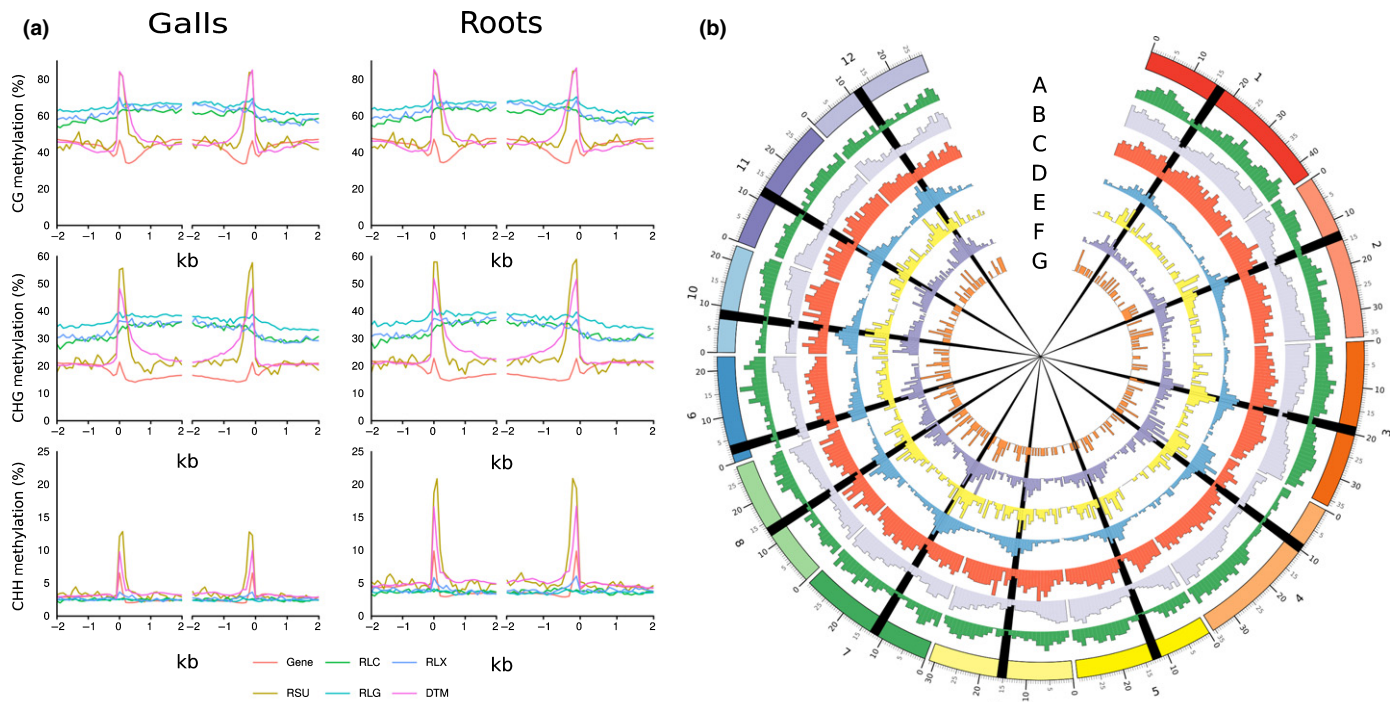


Fig. 3 Overview of promoter/terminator methylation and genome-wide distribution of genomic regions in 3 d post-inoculation (dpi) galls induced by *Meloidogyne graminicola* in rice. (a) DNA methylation of promoter and terminator regions in 3 dpi galls and control root tips, 2 kb upstream and 2 kb downstream from start (left) or end (right), of genes and transposable element (TE) classes RLC, RLG, RLX, RSU, and DTM (bin size of 100 bases). (b) Genome-wide overview. Outer circle represents the 12 rice chromosomes. Black bands represent the centromere regions. Inner circles represent the distribution of differentially methylated regions across the (A) chromosomes, (B) genes, (C) TE class DTM, (D) TE class RLG, (E) TE class RLX, (F) TE class RLC, (G) TE class RSU. DTM, DNA transposon mutator; RLG, Retroelement long tandem repeat Gypsy; RLC, Retroelement long tandem repeat Copia; RLX, Retroelement long tandem repeat 'Unknown'; RSU, Retroelement short interspersed nuclear element.

associated with TEs. However, CHH DMRs are positively associated with DTM ($P < 0.001$) and RSU TEs ($P < 0.001$), and negatively associated with RLC ($P < 0.001$), RLG ($P < 0.001$), RLX ($P < 0.001$) TEs (Fig. 4b). Hypomethylated TEs are significantly enriched in gene promoters for classes DTM ($P < 0.001$), RLC ($P < 0.001$), RLG ($P < 0.001$) and RLX ($P = 0.009$). Genes with TE hypomethylation in their promotor are mainly enriched for GO terms related to plant stress responses and signalling (Figs S5, S6).

DNA hypomethylation correlates with a delayed transcriptional response in gall tissue

Given the prominent presence of CHH hypomethylation in gene promoters, the relationship with gene expression was evaluated using transcriptome data of 3 dpi (young) and 7 dpi (mature) gall tissue, generated in our laboratory under similar experimental conditions (Kyndt *et al.*, 2012; Figs S7, S8). There was no significant overlap between the presence of CG DMRs and DE genes at either 3 or 7 dpi, whether located in promoter or gene body regions. Neither did we find an association between CHH DMRs and gene expression for promoters at 3 dpi, gene body regions at 3 dpi, or gene body regions at 7 dpi. However, 3 dpi CHH DMRs were found to be significantly overrepresented in promoter regions of genes

differentially upregulated at 7 dpi ($P < 0.001$; Fig. 5a,b). Moreover, binomial tests revealed that differential expression at 7 dpi showed significant upregulation in galls, both for all (758 upregulated DE genes/805 DE genes, $P < 2.2 \times 10^{-16}$) DE genes and for the subset associated with CHH DMRs (115 upregulated DE genes/117 DE genes, $P < 2.2 \times 10^{-16}$), whereas this trend was not seen at 3 dpi (66 upregulated DE genes/131 DE genes, $P = 1$). By contrast, no association was found between gene body DMRs at 3 dpi and differential expression at either time point. These data indicate that CHH hypomethylation in gene promoters was associated with gene expression, with a delayed effect of CHH hypomethylation on gene expression activation. For TEs, however, there was no clear association between differential methylation and timing or direction of differential expression (Fig. S9). An overview of TEs/genes that were both differentially methylated and DE can be found in Table S5. Fig. 5(c) illustrates the promoter CHH hypomethylation profile for one of these genes, a locus on chromosome 4, encoding a basic helix–loop–helix (bHLH) transcription factor (Os**bHLH65**), for which gene expression has previously been shown to be suppressed at 3 dpi but activated in 7 dpi galls based on RNA-sequencing (RNA-seq) data (Kyndt *et al.*, 2012). Interestingly, the list of overlapping genes also included eight genes of the ethylene (ET) pathway (e.g. Os04g41570, Os01g54890

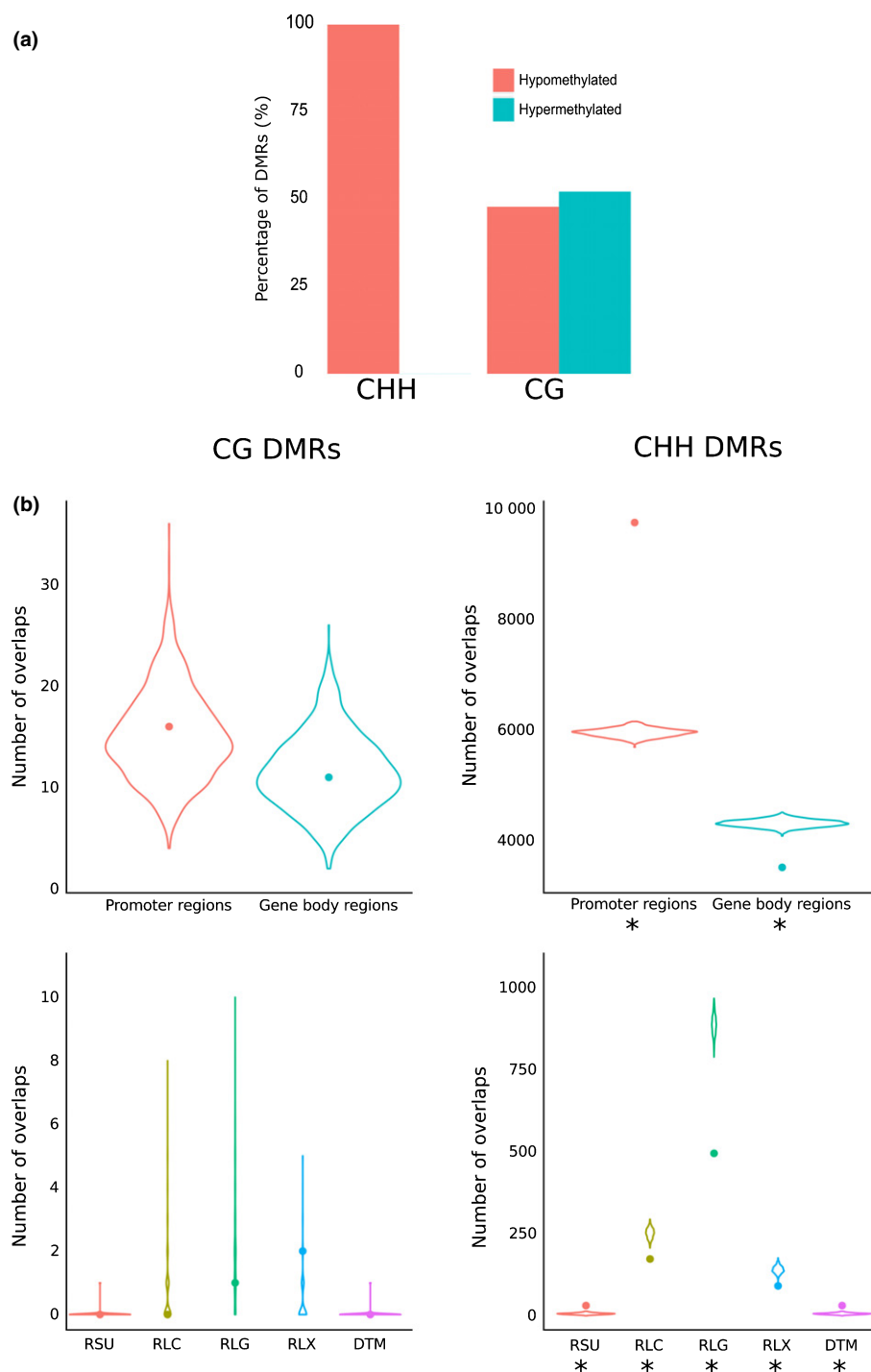


Fig. 4 Differentially methylated regions (DMRs) in 3 d post-inoculation (dpi) galls induced by *Meloidogyne graminicola* in rice. (a) Methylation pattern of DMRs. (b) Significance of associations between DMRs and genomic elements. The violin plots show the distribution of the number of the overlaps between DMRs and randomly scattered transposable element (TE) or gene regions (1000 simulations). The dots show the observed number of overlaps between DMRs and TE gene regions in the whole-genome bisulphite sequencing data set of nematode-induced galls. Asterisks indicate significant over or underrepresentation ($P < 0.05$). DTM, DNA transposon mutator; RLG, Retroelement long tandem repeat Gypsy; RLC, Retroelement long tandem repeat Copia; RLX, Retroelement long tandem repeat 'Unknown'; RSU, Retroelement short interspersed nuclear element.

Os06g29730 and Os04g49194) and a member of the nucleotide binding site leucine-rich repeat family (Os11g45970), known to have a role in plant defence (DeYoung & Innes, 2006; McHale *et al.*, 2006). Delayed activation of five genes with CHH-hypomethylated promoters (Figs 5c, S10) was here independently confirmed by qRT-qPCR on 3 dpi and 7 dpi galls. Confirming RNA-seq data, those genes showed low or repressed expression at 3 dpi and derepression of expression at 7 dpi in gall tissue (Fig. 5d).

RdDM and *DDM1* mutants confirm that DNA methylome changes are involved in plant defence against nematodes

The prominent role of CHH hypomethylation strongly suggests involvement of the *RdDM* pathway or *DDM1* (both of which control CHH methylation) in the plant PTI response upon nematode infection. Further detailed evaluation of previously published transcriptome data of rice upon *M. graminicola* infection (Kyndt *et al.*, 2012; Ji *et al.*, 2013) indeed supports a

transcriptional disturbance of genes related to canonical and non-canonical RdDM pathways and demethylases in this interaction (Fig. S11). Rice mutants in DDM1 and different proteins involved in the RdDM pathway were obtained and infected with root-knot nematodes. In the *dcl3b* mutant line, the number of nematodes significantly decreased by 31.6% compared with the control, whereas the number of galls was also marginally decreased by 12.5% (Fig. 6a). Similarly, in *dcl3a*, decreases of c. 16.1% were observed for both galls and nematodes (Fig. S8a). Rice has two AGO4 orthologues: AGO4a and AGO4b. The double *ago4a/4b* mutant showed a significant decrease in number of galls (36%) and nematodes (35%) (Fig. 6b). A *waf1* mutant, orthologous to *ben1* in Arabidopsis, also showed a slight decline in the number of galls and a significantly lower number of nematodes, with decreases of 16.3% and 18.7%, respectively, compared with wild-type 'Kinmaze' (Fig. 6c). The same observation was made for the *drm2* mutant (Tan *et al.*, 2016), with decreases of 15.3% and 21.9% for galls and nematodes, respectively (Fig. 6d). For the *ddm1a/1b* double mutant (Tan *et al.*, 2016), decreases of 9.47% and 12.33% for galls and nematodes, respectively, were observed compared with their wild-type 'Dongjin' (Fig. S12b). The number of females per gall in control vs mutant lines was not significantly different (except for *ago4ab*) (Fig. S13). These data confirm the role of DNA methylation in mediating early plant immunity of rice to root-knot nematodes and suggest a central role for the RdDM pathway and DDM1 in this process.

Discussion

In this research, we evaluated the hypothesis that DNA hypomethylation is part of a general, conserved PTI response upon recognition of a NAMP in plants. Earlier studies have focused on Arabidopsis and aboveground pathogens, mainly bacteria. Here, we demonstrate that massive DNA hypomethylation occurs early upon nematode infection in rice roots and that hypomethylation can be triggered by treatment with NAMPs, similar to with PAMPs, in both monocot and dicot plants.

Supporting the causal relationship between DNA hypomethylation and plant basal defence responses, genome-wide DNA demethylation by foliar application of 5-azacytidine decreased rice susceptibility to subsequent root-knot nematode infections. Moreover, the observation of reduced nematode presence in roots confirms that this mainly happens at early stages of infection (Fig. 1b). These results are also consistent with previous findings that DNA demethylation hampers the multiplication and vascular accumulation of *P. syringae* in Arabidopsis (Yu *et al.*, 2013), and that a triple Arabidopsis DNA demethylase mutant, *ros1/dml2/dml3*, is more susceptible towards fungal pathogen *F. oxysporum* (Le *et al.*, 2014). Research on Arabidopsis–bacterial interactions has also shown that bacterial PAMP flg22 triggers DNA demethylation (Yu *et al.*, 2013), which was extended here by similar hypomethylation responses in rice and tomato (Fig. 2). The fact that treatment with NAMPs, similar to that described to activate PTI in Arabidopsis (Mendy *et al.*, 2017; De Kesel *et al.*, 2020), as well as flg22 PAMP, induces strong hypomethylation in monocot and dicot plants confirms our hypothesis of DNA

hypomethylation as an evolutionarily conserved PTI response upon infection in plant tissues. We extend previous observations by demonstrating the organ-independent effect (roots in our study vs shoots in other studies) of DNA hypomethylation as a plant immune response.

Moreover, our results indicate a crucial role for promoter CHH methylation in the plant response upon root-knot nematode infection and a delayed effect of the DNA methylation changes on the gene expression profile (Fig. 5d). Even though bisulphite sequencing coverage was relatively low, there was still sufficient power to detect DMRs when differences in methylation were analysed at region level rather than at individual cytosine level. Furthermore, DMRSEQ (v.1.0.14; Korthauer *et al.*, 2018) utilizes a smoothing algorithm to tackle loss of power due to low coverage. Based on the knowledge that the RdDM and DDM1 pathways are the two main mediators of *de novo* and maintenance methylation in CHH context (Law & Jacobsen, 2010; Zemach *et al.*, 2013), we hypothesized that there would be a role for these pathways in rice–*M. graminicola* interaction. This hypothesis was confirmed by minor but consistent reduced susceptibility of RdDM and DDM1-deficient rice mutants (Figs 6, S12b), which are known to have a significant CHH hypomethylation profile (Tan *et al.*, 2016). For example, the *ddm1a/1b* double mutant has 44.9%, 73.5% and 49% less CG, CHG and CHH methylation, respectively, whereas the *drm2* mutant has nearly no CHH DNA methylation (Tan *et al.*, 2016). Our data confirm very recent publications that showed the same trend of enhanced resistance in Arabidopsis RdDM mutants infected with nematodes (Ruiz-Ferrer *et al.*, 2018) or bacterial pathogens (Pavet *et al.*, 2006). The rice *ago4a/4b* double mutant confirmed results for other mutants, in showing a significantly decreased susceptibility to nematode infection (Fig. 6b), yet contrasts with a study on Arabidopsis where enhanced susceptibility to infection by *P. syringae* pv *tomato* DC3000 was observed for this specific mutant (Agorio & Vera, 2007). The authors hypothesized that AGO4 works independently of RdDM in plant disease resistance in Arabidopsis (Agorio & Vera, 2007), but our data did not confirm this in rice. Whereas our data show a context-specific hypomethylation pattern (namely CHH), studies on cyst-nematode-infected Arabidopsis and soybean have described overrepresentation of hypomethylated DMRs in all three cytosine contexts (Rambani *et al.*, 2015; Hewezi *et al.*, 2017). Therefore, though there is clear evidence for the role of DNA hypomethylation in plant defence in all plant kingdoms, additional research is required to evaluate whether the underlying molecular pathways differ between monocots and dicots.

Interestingly, we observed a correlation in expression profile between many ET pathway genes revealing 3 dpi CHH promoter hypomethylation and transcriptional activation/derepression at 7 dpi (Fig. 5d). It has been shown before that ET pathway genes are suppressed upon root-knot nematode infection at 3 dpi and then recovered at 7 dpi in rice (Nahar *et al.*, 2011; Kyndt *et al.*, 2012). Based on the observed correlation in gene expression, we hypothesize that loss of CHH DNA methylation primes the ET-dependent defence response, potentially restricting the parasitic interaction between root-knot nematodes and roots. As reviewed

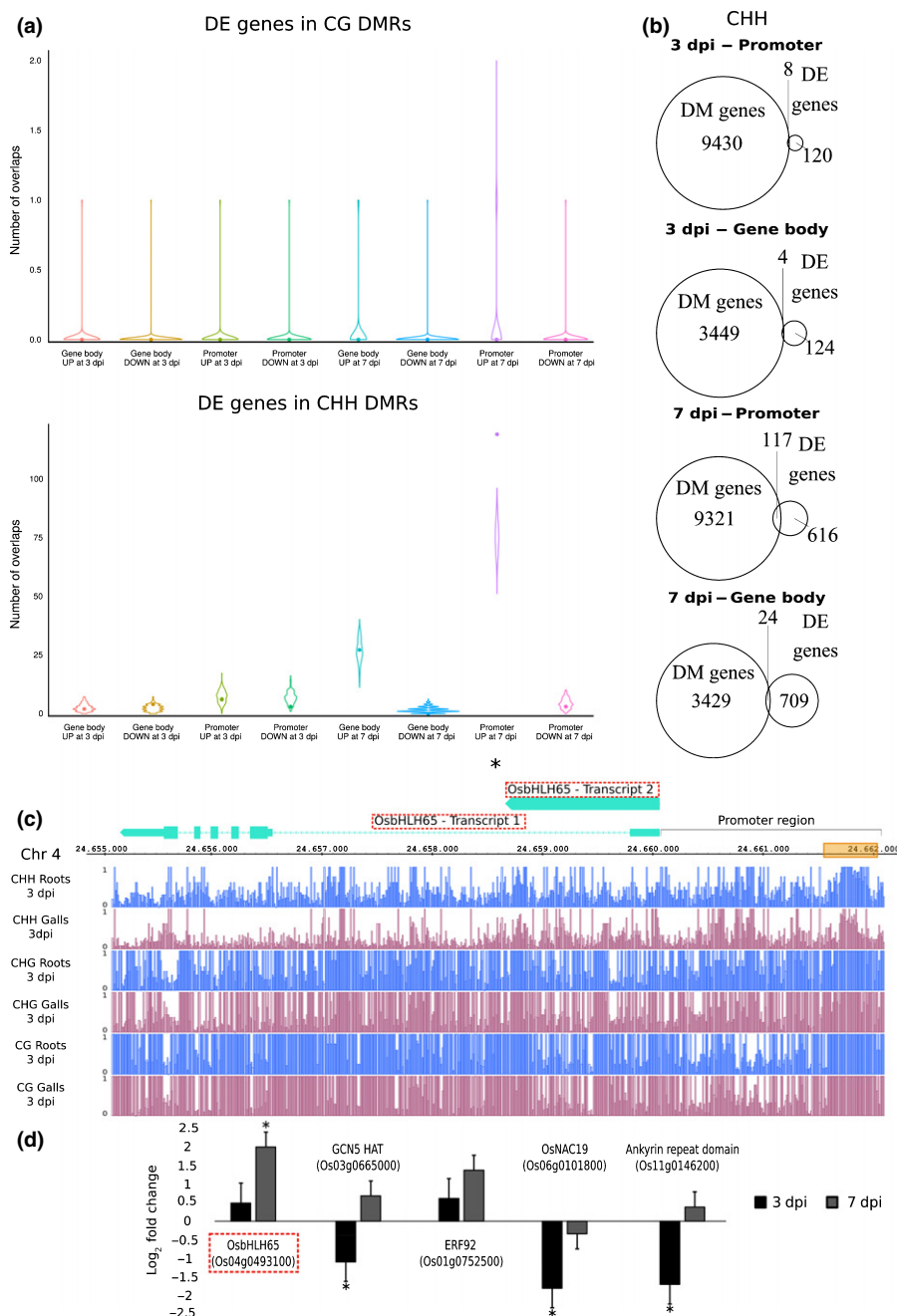


Fig. 5 DNA methylation association with gene expression in galls induced by *Meloidogyne graminicola* in rice. (a) Significance of associations between differentially methylated (DM) regions (DMRs) and differentially expressed (DE) genomic elements. The violin plots show the distribution of overlaps between DMRs and a randomly sampled group of genes/promoters. The dots show the observed number of overlaps between DMRs and DE genes, or promoters of DE genes, in the whole-genome bisulphite sequencing data set of nematode-induced galls. *, $P < 0.05$. (b) Venn diagrams showing the number of genes that overlap with either their gene body or their promoter with 3 d post-inoculation (dpi) CHH DMRs (DM genes) and the number of DE genes at 3 or 7 dpi. (c) DNA methylation at 3 dpi (percentage) in galls and roots for interval 24 655 000–24 662 000 on chromosome 4 (bin size of 100 bases). Note the similar methylation levels between galls and root for CG and CHG methylation, the CHH hypomethylation in the promoter region of gene *OsHAT* at 7 dpi. The DMR is indicated with an orange box. (d) Quantitative reverse transcription PCR-based expression profile of five genes that contain a DMR in their promoter in 3 dpi and 7 dpi gall tissue; *OsHAT* is indicated with a red dashed box. Error bars indicate SEM. *, $P < 0.05$. bHLH, basic helix–loop–helix.

(Kyndt *et al.*, 2013), the ET pathway plays different spatio-temporal roles at different stages of the nematode infection process, including activation of jasmonic-acid-dependent defence responses. Intriguingly, research on fruit ripening has revealed a

similar link between DNA hypomethylation and ET, with, for example, active hypomethylation at the induction of tomato ripening and hypermethylation during maturation of sweet oranges (Lang *et al.*, 2017; Yin *et al.*, 2017; Zuo *et al.*, 2018;

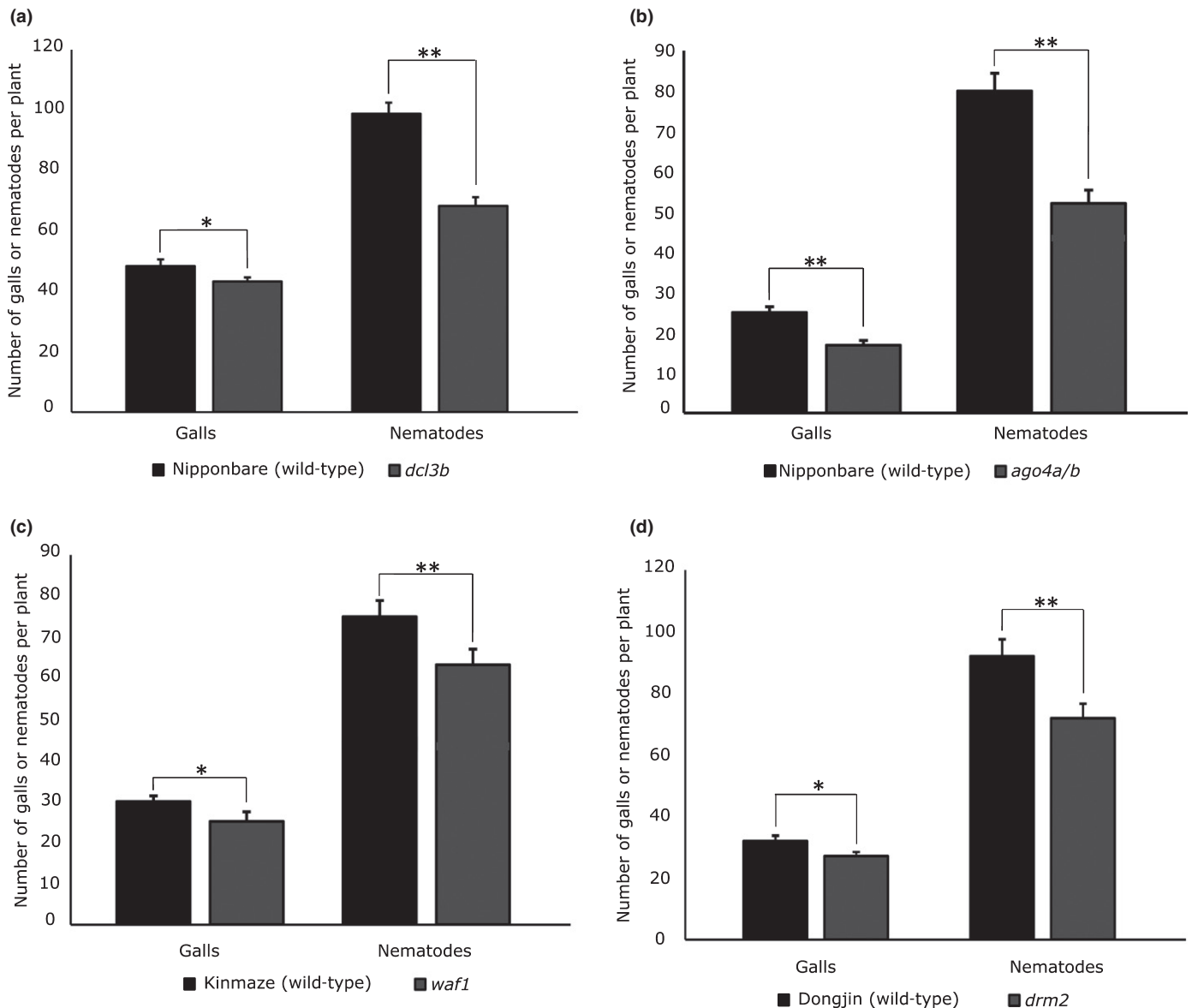


Fig. 6 DNA hypomethylation confers reduced susceptibility to *Meloidogyne graminicola* infection in rice plants. Mutants of (a) DICER-LIKE 3b (*dcl3b*, $n = 20$), (b) ARGONAUTE 4a/b (*ago4a/b*, $n = 19$), (c) WAVY LEAF 1 (*waf1*, $n = 20$). (d) DOMAINS REARRANGED METHYLTRANSFERASE (*drm2*, $n = 23$) are less susceptible to nematode infection. Galls and nematodes were counted 2 wk post-inoculation. *, $P < 0.1$; **, $P < 0.05$. Error bars indicate SEM.

Huang *et al.*, 2019). Whether temporal patterns in DNA methylation also occur during induction or maturation of nematode feeding sites remains to be investigated. Abiotic or biotic stresses have previously been described to awaken dormant TEs in plants (Bouvet *et al.*, 2008; Downen *et al.*, 2012). TE activation can alter gene expression directly (e.g. through insertion in gene body regions or promoters), as for example observed in the promoter of defence genes against *F. oxysporum* (Le *et al.*, 2014) and in resistance gene *Xa21* (Akimoto *et al.*, 2007). However, TEs can also exert indirect effects by generating smRNAs as substrates for DCL proteins to synthesize *trans*-active siRNAs (tasiRNAs) that could potentially silence modulators of plant defence in the same

or distant tissues. The indirect scenario is consistent with accumulation of TE-derived 21 nt siRNAs observed upon salicylate treatment in Arabidopsis (Downen *et al.*, 2012) and 23 or 24 nt repeat-associated and tasiRNA accumulation in galls induced by root-knot nematodes in tomato and Arabidopsis (Medina *et al.*, 2018). This led to the hypothesis that genome fluidity caused by derepression of TEs could permit phenotypic plasticity and adaptation to stress (Negi *et al.*, 2016). We found two TE classes significantly associated with CHH DMRs in 3 dpi galls: RLG (retrotransposon type) and DTM (DNA transposon type) (Fig. S7). However, the low number of overlaps between DE TEs and CHH DMRs, though statistically significant, might not be

biologically relevant. It needs to be further investigated whether the RLG and DTM classes have a specific role in plant adaptation to nematode stress, particularly given that TE derepression (3 dpi) occurs prior to activation of other genes (7 dpi). We detected significant enrichment of hypomethylated TEs in promoters of genes related to plant stress responses and signalling (Figs S5, S6), further endorsing the link between DNA hypomethylation and plant defence.

Finally, it remains to be studied whether changes in DNA methylation are transferred to the next generation of stressed plants. This phenomenon is known as transgenerational acquired resistance and can be triggered by various (a)biotic stresses (Luna *et al.*, 2012; Slaughter *et al.*, 2012). A recent paper found four DNA loci (epigenetic quantitative trait loci, epiQTLs) in *Arabidopsis* in which their heritable hypomethylated state was significantly linked to disease resistance against oomycete *H. arabidopsidis*. These epiQTLs seem to regulate gene expression through trans-regulatory mechanisms (Furci *et al.*, 2019), but have not been investigated in rice.

In summary, our study shows for the first time that massive and genome-wide hypomethylation is part of the PTI response to nematode infection. At least in rice, demethylation is particularly present in the CHH context, and its occurrence in promoters is correlated with derepressed gene expression. Our study, therefore, provides new insights into the general role of DNA demethylation in plant–pathogen interactions across plant kingdoms. Further investigation of the mechanism(s) underlying DNA demethylation is required to obtain a clear insight into how transcriptional and epigenetic reprogramming is obtained during PTI.

Acknowledgements

We would like to thank the persons that kindly provided mutants for infection experiment: Dr Xiaofeng Cao, who provided the *dcl3a* and *dcl3b* mutants; Dr Yijun Qi, who provided the *ago4a/b* double mutant; Feng Tang (from Dr Dao-Xiu Zhou's laboratory), who provided the *drm2* and *ddm1a/b* mutants; and Dr Jun-ichi Itoh, who provided the *waf1* mutant. This work was supported by Fonds Wetenschappelijk Onderzoek (FWO)-Vlaanderen (G007417N) and Bijzonder Onderzoeksfonds UGent (BOF-starting grant). MRA was supported by the Ministry of Science, Research and Technology of Iran. We also thank Richard Raj Singh and Radisras Nkurunziza for technical support. The authors declare that they have no competing interests.

Author contributions

MRA performed the wet-laboratory experiments, under technical support and using protocols as optimized by TK. BV and TDM performed the bio-informatic analyses. MRA and BV wrote the manuscript, with substantial input from TK and TDM. MRA and BV contributed equally to this work. TDM and TK contributed equally to this work.

ORCID

Mohammad Reza Atighi  <https://orcid.org/0000-0003-4510-7891>

Tim De Meyer  <https://orcid.org/0000-0003-2994-9693>

Tina Kyndt  <https://orcid.org/0000-0002-5267-5013>

References

- Abe M, Yoshikawa T, Nosaka M, Sakakibara H, Sato Y, Nagato Y, Itoh J. 2010. *WAVY LEAF1*, an ortholog of *Arabidopsis HEN1*, regulates shoot development by maintaining microRNA and trans-acting small interfering RNA accumulation in rice. *Plant Physiology* 154: 1335–1346.
- Agorio A, Vera P. 2007. ARGONAUTE4 is required for resistance to *Pseudomonas syringae* in *Arabidopsis*. *Plant Cell* 19: 3778–3790.
- Akimoto K, Katakami H, Kim HJ, Ogawa E, Sano CM, Wada Y, Sano H. 2007. Epigenetic inheritance in rice plants. *Annals of Botany* 100: 205–217.
- Bolger AM, Lohse M, Usadel B. 2014. TRIMMOMATIC: a flexible trimmer for Illumina sequence data. *Bioinformatics* 30: 2114–2120.
- Bouvet GF, Jacobi V, Plourde KV, Bernier L. 2008. Stress-induced mobility of *OPHIO1* and *OPHIO2*, DNA transposons of the Dutch elm disease fungi. *Fungal Genetics and Biology* 45: 565–578.
- Bridge J, Plowright RA, Peng D. 2005. Nematode parasites of rice. In: Luc M, Sikora RA, Bridge J, eds. *Plant parasitic nematodes in subtropical and tropical agriculture*. Wallingford, UK: CABI Bioscience, 87–130.
- Cabrera J, Barcala M, Garcia A, Rio-Machin A, Medina C, Jaubert-Possamai S, Favory B, Maizel A, Ruiz-Ferrer V, Fenoll C *et al.* 2016. Differentially expressed small RNAs in *Arabidopsis* galls formed by *Meloidogyne javanica*: a functional role for miR390 and its TAS3-derived tasiRNAs. *New Phytologist* 209: 1625–1640.
- Chan SW, Henderson IR, Jacobsen SE. 2005. Gardening the genome: DNA methylation in *Arabidopsis thaliana*. *Nature Reviews. Genetics* 6: 351–360.
- Copetti D, Zhang J, El Baidouri M, Gao D, Wang J, Barghini E, Cossu RM, Angelova A, Maldonado LC, Roffler S *et al.* 2015. RiTE database: a resource database for genus-wide rice genomics and evolutionary biology. *BMC Genomics* 16: e538.
- Dasgupta P, Chaudhuri S. 2019. Analysis of DNA methylation profile in plants by chop-PCR. In: Gassmann W, ed. *Plant innate immunity: methods and protocols. Methods in Molecular Biology*, vol. 1991. New York, NY, USA: Humana, 79–90.
- De Kesel J, Gómez-Rodríguez R, Bonneure E, Mangelinckx S, Kyndt T. 2020. The use of PTI-marker genes to identify novel compounds that establish induced resistance in rice. *International Journal of Molecular Sciences* 21: e317.
- Deleris A, Halter T, Navarro L. 2016. DNA methylation and demethylation in plant immunity. *Annual Review of Phytopathology* 54: 579–603.
- DeYoung BJ, Innes RW. 2006. Plant NBS-LRR proteins in pathogen sensing and host defense. *Nature Immunology* 7: 1243–1249.
- Dobin A, Davis CA, Schlesinger F, Drenkow J, Zaleski C, Jha S, Batut P, Chaisson M, Gingeras TR. 2013. STAR: ultrafast universal RNA-seq aligner. *Bioinformatics* 29: 15–21.
- Downen RH, Pelizzola M, Schmitz RJ, Lister R, Downen JM, Nery JR, Dixon JE, Ecker JR. 2012. Widespread dynamic DNA methylation in response to biotic stress. *Proceedings of the National Academy of Sciences, USA* 109: E2183–2191.
- Doyle JJ, Doyle JL. 1987. A rapid DNA isolation procedure for small quantities of fresh leaf tissue. *Phytochemical Bulletin* 19: 11–15.
- Furci L, Jain R, Stassen J, Berkowitz O, Whelan J, Roquis D, Baillet V, Colot V, Johannes F, Ton J. 2019. Identification and characterisation of hypomethylated DNA loci controlling quantitative resistance in *Arabidopsis*. *eLife* 8: e40655.
- Gel B, Diez-Villanueva A, Serra E, Buschbeck M, Peinado MA, Malinverni R. 2016. REGIONER: an R/BIOCONDUCTOR package for the association analysis of genomic regions based on permutation tests. *Bioinformatics* 32: 289–291.

- Gonzalez AP, Chrtjek J, Dobrev PI, Dimalasova V, Fehrer J, Mraz P, Latzel V. 2016. Stress-induced memory alters growth of clonal offspring of white clover (*Trifolium repens*). *American Journal of Botany* 103: 1567–1574.
- Haag JR, Pikaard CS. 2011. Multisubunit RNA polymerases IV and V: purveyors of non-coding RNA for plant gene silencing. *Nature reviews. Molecular Cell Biology* 12: 483–492.
- Hewezi T, Howe P, Maier TR, Baum TJ. 2008. Arabidopsis small RNAs and their targets during cyst nematode parasitism. *Molecular Plant–Microbe Interactions* 21: 1622–1634.
- Hewezi T, Lane T, Piya S, Rambani A, Rice JH, Staton M. 2017. Cyst nematode parasitism induces dynamic changes in the root epigenome. *Plant Physiology* 174: 405–420.
- Huang H, Liu R, Niu Q, Tang K, Zhang B, Zhang H, Chen K, Zhu JK, Lang Z. 2019. Global increase in DNA methylation during orange fruit development and ripening. *Proceedings of the National Academy of Sciences, USA* 116: 1430–1436.
- Ji H, Gheysen G, Denil S, Lindsey K, Topping JF, Nahar K, Haegeman A, De Vos WH, Trooskens G, Van Criekinge W *et al.* 2013. Transcriptional analysis through RNA sequencing of giant cells induced by *Meloidogyne graminicola* in rice roots. *Journal of Experimental Botany* 64: 3885–3898.
- Jones JD, Dangl JL. 2006. The plant immune system. *Nature* 444: 323–329.
- Khanam S, Bauters L, Singh RR, Verbeek R, Haack A, Sultan SMD, Demeestere K, Kyndt T, Gheysen G. 2018. Mechanisms of resistance in the rice cultivar Manikpukha to the rice stem nematode *Ditylenchus angustus*. *Molecular Plant Pathology* 19: 1391–1402.
- Korthauer K, Chakraborty S, Benjamini Y, Izaray RA. 2018. Detection and accurate false discovery rate control of differentially methylated regions from whole genome bisulfite sequencing. *Biostatistics* 20: 367–383.
- Krueger F, Andrews SR. 2011. BISMARCK: a flexible aligner and methylation caller for bisulfite-seq applications. *Bioinformatics* 27: 1571–1572.
- Kyndt T, Denil S, Haegeman A, Trooskens G, Bauters L, Van Criekinge W, De Meyer T, Gheysen G. 2012. Transcriptional reprogramming by root knot and migratory nematode infection in rice. *New Phytologist* 196: 887–900.
- Kyndt T, Vieira P, Gheysen G, de Almeida-Engler J. 2013. Nematode feeding sites: unique organs in plant roots. *Planta* 238: 807–818.
- Lang Z, Wang Y, Tang K, Tang D, Datsenko T, Cheng J, Zhang Y, Handa AK, Zhu JK. 2017. Critical roles of DNA demethylation in the activation of ripening-induced genes and inhibition of ripening-repressed genes in tomato fruit. *Proceedings of the National Academy of Sciences, USA* 114: E4511–e4519.
- Latzel V, Rendina González AP, Rosenthal J. 2016. Epigenetic memory as a basis for intelligent behavior in clonal plants. *Frontiers in Plant Science* 7: e1354.
- Law JA, Jacobsen SE. 2010. Establishing, maintaining and modifying DNA methylation patterns in plants and animals. *Nature Reviews Genetics* 11: 204–220.
- Lawrence M, Huber W, Pages H, Aboyoun P, Carlson M, Gentleman R, Morgan MT, Carey VJ. 2013. Software for computing and annotating genomic ranges. *PLoS Computational Biology* 9: e1003118.
- Le TN, Schumann U, Smith NA, Tiwari S, Au PC, Zhu QH, Taylor JM, Kazan K, Llewellyn DJ, Zhang R *et al.* 2014. DNA demethylases target promoter transposable elements to positively regulate stress responsive genes in *Arabidopsis*. *Genome Biology* 15: e458.
- Li X, Wang X, Zhang S, Liu D, Duan Y, Dong W. 2012. Identification of soybean microRNAs involved in soybean cyst nematode infection by deep sequencing. *PLoS ONE* 7: e39650.
- Lisch D. 2009. Epigenetic regulation of transposable elements in plants. *Annual Review of Plant Biology* 60: 43–66.
- López Sánchez A, Stassen JH, Furci L, Smith LM, Ton J. 2016. The role of DNA (de)methylation in immune responsiveness of *Arabidopsis*. *The Plant Journal* 88: 361–374.
- Love MI, Huber W, Anders S. 2014. Moderated estimation of fold change and dispersion for RNA-seq data with DESeq2. *Genome Biology* 15: e550.
- Luna E, Bruce TJ, Roberts MR, Flors V, Ton J. 2012. Next-generation systemic acquired resistance. *Plant Physiology* 158: 844–853.
- Mantelin S, Bellafiore S, Kyndt T. 2017. *Meloidogyne graminicola*: a major threat to rice agriculture. *Molecular Plant Pathology* 18: 3–15.
- Matzke MA, Mosher RA. 2014. RNA-directed DNA methylation: an epigenetic pathway of increasing complexity. *Nature Reviews Genetics* 15: 394–408.
- McHale L, Tan X, Koehl P, Michelmore RW. 2006. Plant NBS-LRR proteins: adaptable guards. *Genome Biology* 7: e212.
- Medina C, da Rocha M, Magliano M, Raptopoulou A, Marteu N, Lebrigand K, Abad P, Favery B, Jaubert-Possamai S. 2018. Characterization of siRNAs clusters in *Arabidopsis thaliana* galls induced by the root-knot nematode *Meloidogyne incognita*. *BMC Genomics* 19: e943.
- Mendy B, Wang'ombe MW, Radakovic ZS, Holbein J, Ilyas M, Chopra D, Holton N, Zipfel C, Grundler FM, Siddique S. 2017. Arabidopsis leucine-rich repeat receptor-like kinase NLR1 is required for induction of innate immunity to parasitic nematodes. *PLoS Pathogens* 13: e1006284.
- Mi H, Huang X, Muruganujan A, Tang H, Mills C, Kang D, Thomas PD. 2017. PANTHER version 11: expanded annotation data from gene ontology and reactome pathways, and data analysis tool enhancements. *Nucleic Acids Research* 45: D183–D189.
- Münzbergová Z, Latzel V, Šurinová M, Hadincová V. 2019. DNA methylation as a possible mechanism affecting ability of natural populations to adapt to changing climate. *Oikos* 128: 124–134.
- Nahar K, Kyndt T, De Vleeschauwer D, Hofte M, Gheysen G. 2011. The jasmonate pathway is a key player in systemically induced defense against root knot nematodes in rice. *Plant Physiology* 157: 305–316.
- Negi P, Rai AN, Suprasanna P. 2016. Moving through the stressed genome: emerging regulatory roles for transposons in plant stress responses. *Frontiers in Plant Science* 7: e1448.
- Pavet V, Quintero C, Cecchini NM, Rosa AL, Alvarez ME. 2006. Arabidopsis displays centromeric DNA hypomethylation and cytological alterations of heterochromatin upon attack by *Pseudomonas syringae*. *Molecular Plant–Microbe Interactions* 19: 577–587.
- Pikaard CS, Mittelsten Scheid O. 2014. Epigenetic regulation in plants. *Cold Spring Harbor Perspectives in Biology* 6: a019315.
- Portillo M, Cabrera J, Lindsey K, Topping J, Andres MF, Emiliozzi M, Oliveros JC, Garcia-Casado G, Solano R, Koltai H *et al.* 2013. Distinct and conserved transcriptomic changes during nematode-induced giant cell development in tomato compared with Arabidopsis: a functional role for gene repression. *New Phytologist* 197: 1276–1290.
- Puy J, Dvořáková H, Carmona CP, de Bello F, Hiiesalu I, Latzel V. 2018. Improved demethylation in ecological epigenetic experiments: testing a simple and harmless foliar demethylation application. *Methods in Ecology and Evolution* 9: 744–753.
- Rambani A, Rice JH, Liu J, Lane T, Ranjan P, Mazarei M, Pantalone V, Stewart CN Jr, Staton M, Hewezi T. 2015. The methylome of soybean roots during the compatible interaction with the soybean cyst nematode. *Plant Physiology* 168: 1364–1377.
- Reversat G, Boyer J, Sannier C, Pando-Bahuon AJN. 1999. Use of a mixture of sand and water-absorbent synthetic polymer as substrate for the xenotransferring of plant-parasitic nematodes in the laboratory. *Nematology* 1: 209–212.
- Ruiz-Ferrer V, Cabrera J, Martinez-Argudo I, Artaza H, Fenoll C, Escobar C. 2018. Silenced retrotransposons are major rasiRNAs targets in Arabidopsis galls induced by *Meloidogyne javanica*. *Molecular Plant Pathology* 19: 2431–2445.
- Sasser JN, Carter CC. 1985. Overview of the international *Meloidogyne* project 1975–1984. In: Barker KR, Sasser JN, Carter CC, eds. *An advanced treatise on Meloidogyne, vol. I: biological control*. Raleigh, NC, USA: North Carolina State University and United States Agency for International Development, 19–24.
- Slaughter A, Daniel X, Flors V, Luna E, Hohn B, Mauch-Mani B. 2012. Descendants of primed Arabidopsis plants exhibit resistance to biotic stress. *Plant Physiology* 158: 835–843.
- Slotkin RK, Martienssen R. 2007. Transposable elements and the epigenetic regulation of the genome. *Nature Reviews Genetics* 8: 272–285.
- Somvanshi VS, Tathode M, Shukla RN, Rao U. 2018. Nematode genome announcement: a draft genome for rice root-knot nematode, *Meloidogyne graminicola*. *Journal of Nematology* 50: 111–116.
- Song X, Li P, Zhai J, Zhou M, Ma L, Liu B, Jeong DH, Nakano M, Cao S, Liu C *et al.* 2012. Roles of DCL4 and DCL3b in rice phased small RNA biogenesis. *The Plant Journal* 69: 462–474.

- Supek F, Bosnjak M, Skunca N, Smuc T. 2011. REVIGO summarizes and visualizes long lists of Gene Ontology terms. *PLoS ONE* 6: e21800.
- Tan F, Zhou C, Zhou Q, Zhou S, Yang W, Zhao Y, Li G, Zhou DX. 2016. Analysis of chromatin regulators reveals specific features of rice DNA methylation pathways. *Plant Physiology* 171: 2041–2054.
- Thimm O, Blasing O, Gibon Y, Nagel A, Meyer S, Kruger P, Selbig J, Muller LA, Rhee SY, Stitt M. 2004. MAPMAN: a user-driven tool to display genomics data sets onto diagrams of metabolic pathways and other biological processes. *The Plant Journal* 37: 914–939.
- Tian T, Liu Y, Yan H, You Q, Yi X, Du Z, Xu W, Su Z. 2017. AGRIGO v2.0: a GO analysis toolkit for the agricultural community, 2017 update. *Nucleic Acids Research* 45: W122–W129.
- Wu L, Zhou H, Zhang Q, Zhang J, Ni F, Liu C, Qi Y. 2010. DNA methylation mediated by a microRNA pathway. *Molecular Cell* 38: 465–475.
- Yin Y, Morgunova E, Jolma A, Kaasinen E, Sahu B, Khund-Sayeed S, Das PK, Kivioja T, Dave K, Zhong F, *et al.* 2017. Impact of cytosine methylation on DNA binding specificities of human transcription factors. *Science* 356. doi: 10.1126/science.aaj2239.
- Yu A, Lepere G, Jay F, Wang J, Bapaume L, Wang Y, Abraham AL, Penterman J, Fischer RL, Voinnet O *et al.* 2013. Dynamics and biological relevance of DNA demethylation in *Arabidopsis* antibacterial defense. *Proceedings of the National Academy of Sciences, USA* 110: 2389–2394.
- Zakrzewski F, Schmidt M, Van Lijsebettens M, Schmidt T. 2017. DNA methylation of retrotransposons, DNA transposons and genes in sugar beet (*Beta vulgaris* L.). *The Plant Journal* 90: 1156–1175.
- Zemach A, Kim MY, Hsieh PH, Coleman-Derr D, Eshed-Williams L, Thao K, Harmer SL, Zilberman D. 2013. The *Arabidopsis* nucleosome remodeler DDM1 allows DNA methyltransferases to access H1-containing heterochromatin. *Cell* 153: 193–205.
- Zhang H, Lang Z, Zhu J-K. 2018. Dynamics and function of DNA methylation in plants. *Nature Reviews Molecular Cell Biology* 19: 489–506.
- Zhou M, Palanca AMS, Law JA. 2018. Locus-specific control of the *de novo* DNA methylation pathway in *Arabidopsis* by the CLASSY family. *Nature Genetics* 50: 865–873.
- Zipfel C. 2014. Plant pattern-recognition receptors. *Trends in Immunology* 35: 345–351.
- Zuo J, Wang Y, Zhu B, Luo Y, Wang Q, Gao L. 2018. Comparative analysis of DNA methylation reveals specific regulations on ethylene pathway in tomato fruit. *Genes* 9: e266.

Supporting Information

Additional Supporting Information may be found online in the Supporting Information section at the end of the article.

Fig. S1 Foliar application of 5-Azacytidine (75 μ M) 24 h before nematode inoculation.

Fig. S2 5-Azacytidine treatment causes strong hypomethylation in rice.

Fig. S3 Number of females divided by the number of galls for each treatment.

Fig. S4 Gene ontology of genes that overlap with DMRs.

Fig. S5 Significance of associations between hypomethylated TEs and promoters.

Fig. S6 GO enrichment analysis of genes with a hypomethylated TE in their promotor.

Fig. S7 Venn diagrams showing the number of differentially expressed TEs/genes at either 3 dpi or 7 dpi and differentially methylated TEs/genes (in CG context).

Fig. S8 Venn diagrams showing the number of differentially expressed TEs/genes at either 3 dpi or 7 dpi and differentially methylated TEs/genes (in CHH context).

Fig. S9 Significance of associations between DMRs and differentially expressed TEs.

Fig. S10 DNA methylation at 3 dpi (percentage) in galls and control root tips in CG, CHG and CHH contexts.

Fig. S11 Expression profile of genes involved in DNA methylation upon nematode infection in galls at 3 dpi.

Fig. S12 Susceptibility of rice mutants to nematode infection.

Fig. S13 Comparison of number of females divided by number of galls for each mutant.

Table S1 Overview of read counts per sample after trimming and mapping as well as bisulphite conversion efficiencies.

Table S2 Overview of primers used.

Table S3 ROS quantification upon application of NemaWater.

Table S4 Validation of results obtained by WGBS by ChIP-qPCR.

Table S5 Overview of genes that show overlap with differentially methylated regions.

Table S6 Genome location and statistics of the differentially methylated regions.

Please note: Wiley Blackwell are not responsible for the content or functionality of any Supporting Information supplied by the authors. Any queries (other than missing material) should be directed to the *New Phytologist* Central Office.